communications materials

Article

https://doi.org/10.1038/s43246-024-00640-y

Mechanical force-switchable aqueous organocatalysis

Nikita Das & Chandan Maity

Control over the catalytic activity of artificial catalytic systems in aqueous media is of high interest for biomimetic artificial catalysts. The activity of catalytic systems can be controlled via introducing stimuli-responsive feature in the structure of the catalytic systems. However, temperature, pH or light have been predominantly used as stimulus. Aqueous catalytic system whose activity can be turned 'ON/OFF' employing mechanical force has not been demonstrated. Here we show how catalytic activity of an aqueous catalytic system can be switched 'ON/OFF' via the application/ceasing ultrasound stimulus. We demonstrate that the accessibility of imidazole, a catalyst moiety, can be modulated via the presence/absence of the ultrasound stimulus, resulting temporal control over the rate of ester hydrolysis reactions in aqueous buffer solution. This generic approach enables using a large range of organocatalysts for the preparation of molecules and/or materials in aqueous media for their application to material science, and in biomedical field.

Catalysis is the key to the synthesis of high-value functional molecules and materials from the readily available building blocks. In nature, enzyme often acts as catalyst for the localized formation of molecules and supramolecular architectures for achieving homeostasis, signalling processes, and motility. Control over catalytic activity is the basis of cellular communication and the regulation of a wide range of biological processes[1,2]In comparison, catalyst has been extensively used in artificial systems for the synthesis of both simple and highly complex molecules. However, catalysis in these systems has been taken place according to the initially chosen reaction conditions. Hence, they lack the control over substrate(s) to product(s) conversion at desired time and place, which is necessary for smart applications[3–5]Besides, catalytic reactions are mainly taking place in organic solvents, which may have adverse environmental impact[6,7]In this regard, water is the eco-friendliest solvent and aqueous chemical reactions can take place in an environmentally friendly means.

Mimicking enzymatic reactions and organocatalytic reactions in aqueous medium have been reported[8,9]. These catalytic systems encounter considerable challenges in aqueous media such as poor reactant solubility, and poor stability of the reaction intermediates. However, only few examples of aqueous organocatalytic systems with switchable catalytic activity exist in literature[10]. This has achieved employing stimuli-responsive catalysts, where catalytic activity can be switched 'ON/OFF' via the application of the stimulus or ceasing it. These catalyst systems contain smart structural features that modulate the reaction rate reversibly according to the presence/absence of stimuli. Example of switchable catalyst activity are predominately controlled by temperature[11–13], pH[14–16]and light[17–23] as stimulus. However, switching the catalytic activity in aqueous media using mechanical force is unknown. Use of mechanical force for switching the catalytic activity in water could be different from thermal, pH or light-induced modulation of catalytic activity[24,25]. Employing ultrasound is one of the efficient ways for mechanical force-induced catalyst activation via polymer chains uncoil and stretch causing the weakest bonds in the chain to rupture[26–28]. Ultrasonic chain scission of polymers has been achieved for various applications ranging from sensing to targeted site-specific drug delivery[29–34]. There has not been any report of switchable organocatalytic activity modulated reversibly with ultrasound stimulus in aqueous media. Here, this work demonstrates an ultrasound-regulated switchable organocatalytic system in aqueous media. The catalytic activity could be turned 'ON' in presence of ultrasound stimulus (switch 'ON'), whereas there would be no catalytic activity in absence of the stimulus (switch 'OFF') (Fig. 1a). The catalytic system comprises an alginate-based material providing imidazole functional group as an organocatalytic moiety for 'on-demand' hydrolysis reaction of active esters (Fig. 1b). Reversible modulation of the catalytic activity has been observed by switching the ultrasound stimulus 'ON/OFF'.

Results

To achieve reversible control over aqueous organocatalysis via the application of ultrasound stimulus, we have considered the following factors:

(a) attachment of an organocatalytic moiety to an ultrasound-responsive material for selective catalyst availability. Ultrasound-induced

(Organic)Material Science and Engineering Laboratory, Department of Chemistry and Centre for Nanobiotechnology (CNBT), Vellore Institute of Technology (VIT), Vellore campus, Tamil Nadu, India. e-mail: chandan.maity@vit.ac.in

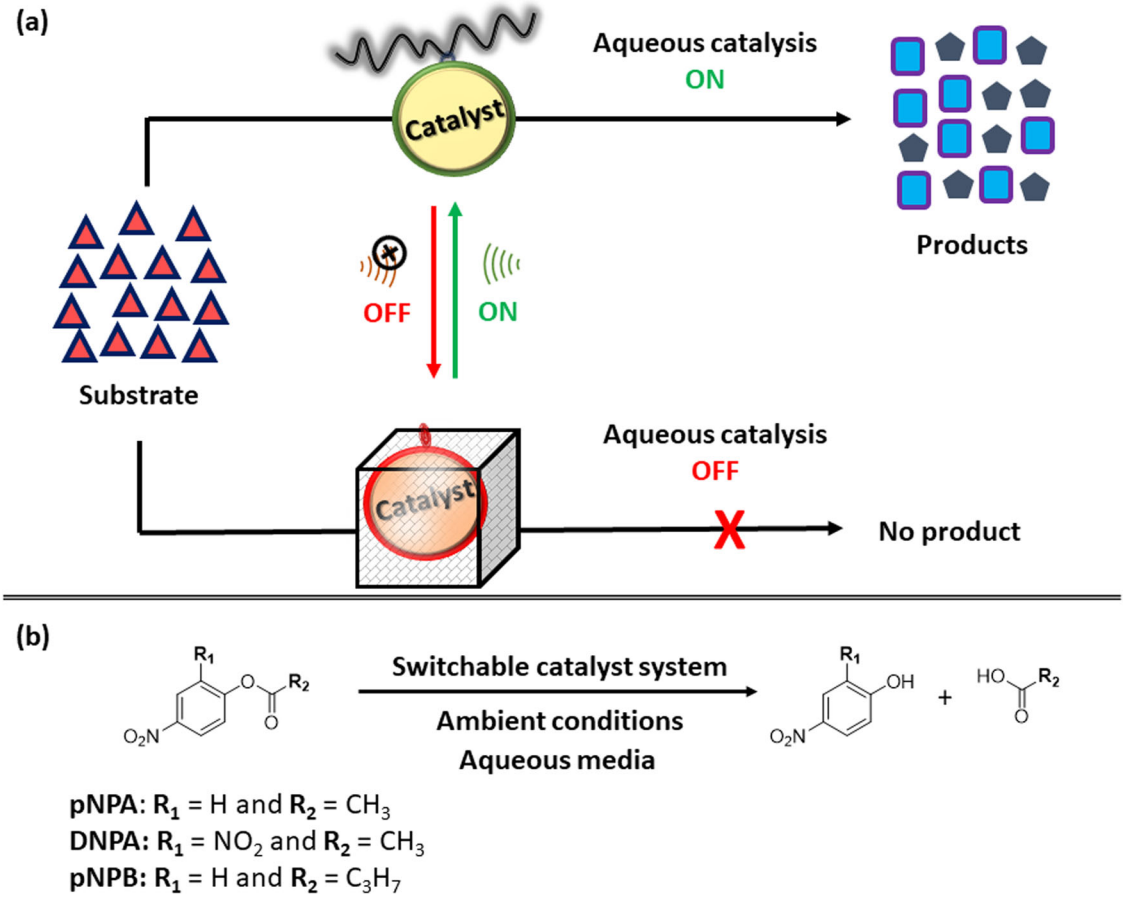

Fig. 1 | A schematic for mechanical force-switchable aqueous organocatalysis. **a** 'ON/OFF' switching of an organocatalyst system in the presence/absence of ultrasound stimuli leading to controlled products formation from the reactant. Presence of ultrasound stimulus allowed accessibility of an organocatalyst for the chemical reaction (catalysis ON), whereas the catalyst system would be inaccessible for the substrate in the absence of the stimulus (catalysis OFF). **b** Ester (pNPA, DNPA, and pNPB) hydrolysis reactions are modulated by the switchable catalyst system in aqueous media at ambient conditions.

mechanical force should be transferred to the catalyst system in a controlled manner, resulting mechanical scission of the system and availability of the organocatalytic moiety. This way, the ultrasound trigger would switch 'ON' the catalytic system.

(b) the stimulus would be inherent towards the catalytic activation only and would not contribute towards the chemical reaction, and

(c) the catalyst moiety would be unavailable towards reactant(s) in the absence of the stimulus. Ceasing the ultrasound stimulus, the catalytic system would return to the original state and thus catalysis would be switched 'OFF'.

Based on these considerations, we have chosen sodium alginate as ultrasound-responsive material as alginate forms hydrogel network in the presence of divalent cations such as Ca^{+2} ion and undergoes gel → sol conversion on exposure to ultrasound stimulus[35–38]. The carboxyl groups of the alginate chain, particularly from the guluronate (G) unit, coordinates with Ca^{+2} ions to form stable hydrogel network via the formation of an "egg-box" model through cooperative interaction of Ca^{+2} ions and the carboxyl groups[39]. Application of ultrasound in aqueous solution of alginate material can produce shear forces around collapsing cavitation bubbles that can influence alginate chains to stretch, and eventually disrupt the coordination bond and crosslinking[37,38].

Ultrasound-induced aqueous organocatalysis

Properties of the alginate-based hydrogel material such as mechanical strength, and morphology depend on molecular weight, ratio of mannuronates and guluronates unit, source of alginate, concentration of crosslinking ions, pH of the media etc.[37,40]. Using $CaCl_2$ as crosslinking agent, we found that minimum of 30 mM $CaCl_2$ is required to obtain alginate hydrogel material (bead) with 3 wt% sodium alginate (Supplementary Table S1). We envisioned that an organocatalyst could be easily encapsulated within alginate hydrogel network just by mixing (via non-covalent attachment) the organocatalyst with sodium alginate prior to hydrogel material preparation. The encapsulated-catalyst would be available for catalysis via disruption of the hydrogel network with ultrasound stimulus (Fig. 2a). Towards this, we found a minimum of 35 mM of Ca^{+2} ion is required to obtain a stable hydrogel material via mixing imidazole (as an organocatalyst) with alginate solution. We used 40 mM of Ca^{+2} ion to prepare alginate hydrogel material ensuring a hydrogel material (Im in Alg) that can withstand minor mechanical forces (such as touching, holding or transporting vial to different place) (Supplementary Table S2). We found that maximum storage modulus (G'_{max}) of alginate hydrogel material (3 wt% sodium alginate with 40 mM of Ca^{+2} ion) was 73.8 kPa, while alginate mixed with imidazole (Im in Alg, 3wt % sodium alginate and 1 mM of imidazole with 40 mM of Ca^{+2} ion) was 14.1 kPa (Supplementary Fig. S4a, b). Influence of the entrapped molecules to the coordination site of the alginate chains is evident from the rheology measurement and from the requirement of higher concentration of crosslinking ions for stable alginate hydrogel material[37,41]. The microscopic structure of the alginate material (Im in Alg) was observed in field emission scanning electron microscopic (FESEM) image showing a rough surface with cube-shaped morphology visible at higher magnifications (Supplementary Fig. S3a, b). Application of ultrasound stimulus resulted dispersion of the beads

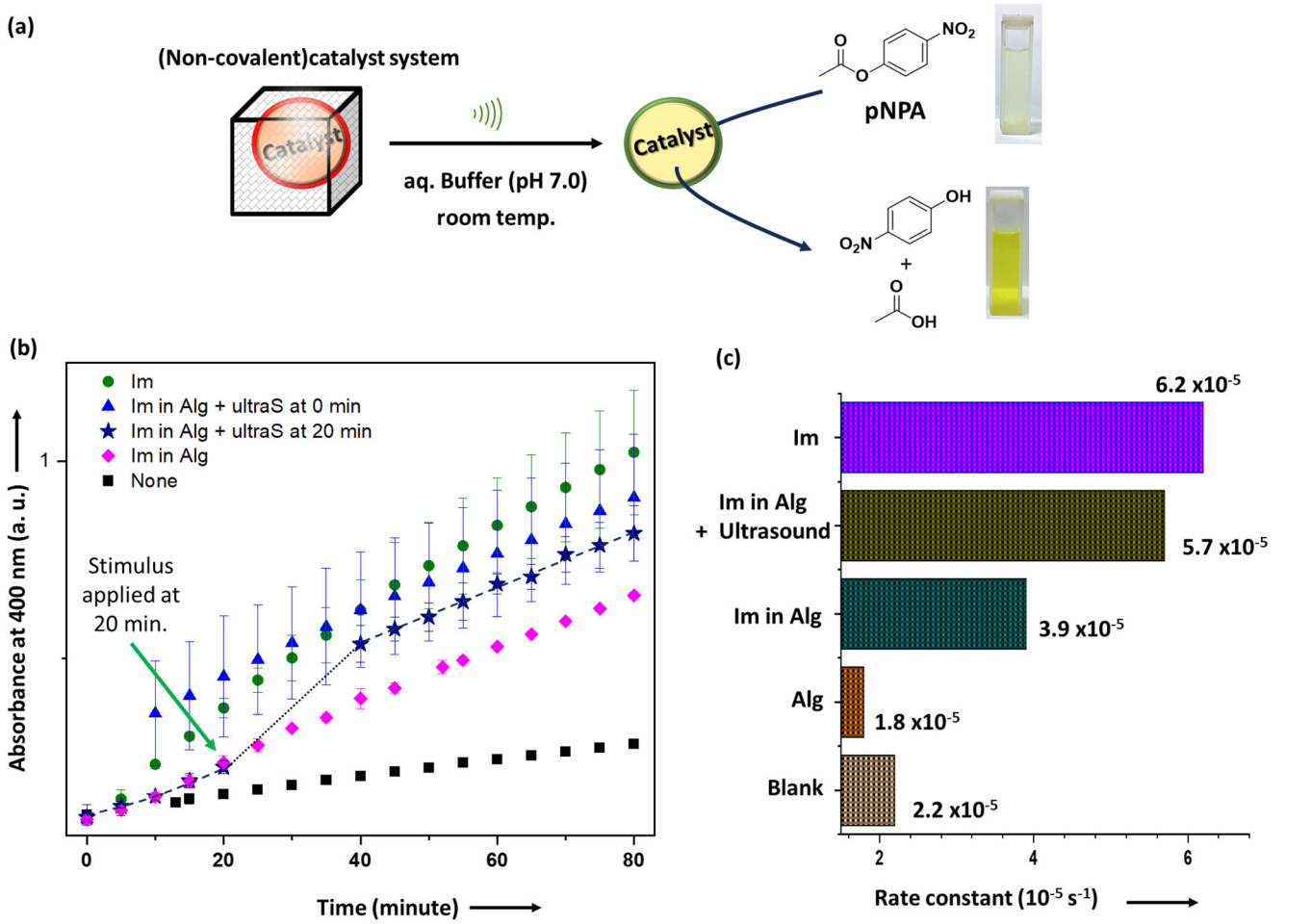

Fig. 2 | Ultrasound-triggered organocatalysis using (non-covalent)catalyst system. a A schematic of catalyst release from the catalyst system via the application of ultrasound stimulus for pNPA hydrolysis to 4-nitrophenol and acetic acid in aqueous buffer at pH = 7.0. Visual colour change (colourless to yellow) is observed due to the formation of 4-nitrophenol. **b** Conversion of the hydrolysis reaction of pNPA in aqueous buffer (pH = 7.0) followed by UV-Vis spectroscopy in the presence of imidazole (green circle), none (black square), imidazole in alginate bead (magenta diamond), imidazole in alginate bead and ultrasound stimulus (blue triangle), and in presence of imidazole in alginate bead without ultrasound stimulus for 20 min and ultrasound stimulus was added after 20 min (navy blue star). Markers indicates the experimental data. Error bars are based on standard errors in duplicate runs. The lines are to guide the eyes. **c** Reaction rate constants at different condition involving (non-covalent) catalyst system.

as a viscous solution, indicating de-crosslinking of the alginate chains in the presence of ultrasound as stimulus. This is in agreement with the finding for ultrasound-triggered disruption of alginate material[38]. Next, we applied ultrasound stimulus to the alginate material and examined ultrasound-induced imidazole catalysis for the hydrolysis of *para*-nitrophenyl acetate (pNPA) in aqueous medium (Fig. 2a). We choose imidazole as organocatalyst as it is widely used as nucleophilic catalyst in synthetic chemistry[42,43], and in biological systems[44,45]. Ultrasound-induced imidazole catalysed pNPA hydrolysis was performed in aqueous buffer solution (1:9 DMF/HEPES buffer, pH = 7.0), DMF is employed to improve the solubility of pNPA substrate in the aqueous solution[46,47]. The reaction provided yellow coloured product (4-nitrophenol) from colourless pNPA that can be followed by recording the absorbance at 400 nm (Fig. 2b). As the reaction progressed, a pseudo-first order kinetics was observed with an increase in absorbance at 400 nm (Kinetic analysis in supplementary). In the absence of imidazole catalyst (black square, Fig. 2b), the reaction rate was $1.8 \times 10^{-5}\ s^{-1}$ (Fig. 2c), whereas the reaction was 3.5-fold faster in the presence of native imidazole (rate = $6.2 \times 10^{-5}\ s^{-1}$). Interestingly, in the presence of ultrasound stimulus, the reaction rate was 3.3-fold higher (rate = $5.7 \times 10^{-5}\ s^{-1}$), which is comparable to the native imidazole catalysis (Fig. 2c). It is worth noting that a probe sonicator was used for creating ultrasonic wave to the reaction mixture for 5 min (Supplementary Table S3 for optimization). Ambient conditions (25–30 °C) were maintained during and after the sonication cycles using inbuilt water bath and temperature sensor and replacing water in regular time interval (Methods section, *vide infra*). Comparable reaction rate indicates the release of imidazole molecule from the alginate hydrogel network to the reaction medium due to the application of ultrasound stimulus. Importantly, the application of ultrasound stimulus during the course of the reaction also could free the imidazole from the reaction environment. To investigate this, we followed the reaction for 20 min, and then ultrasound stimulus was applied (navy blue star). We observed that during the first 20 min, the reaction rate was similar as the background reaction, whereas after the application of ultrasound stimulus, a similar trend to that of the catalysed conditions was observed. This demonstrated an autonomous availability of the catalyst for the substrate to the ultrasound stimulus. However, in the absence of stimulus, an increase in reaction rate (rate = $3.9 \times 10^{-5}\ s^{-1}$, Fig. 2c) was observed only employing alginate hydrogel bead containing imidazole (magenta diamond). A 2.2-fold higher rate can be ascribed to the diffusional escape of imidazole from the alginate hydrogel bead to the reaction medium.

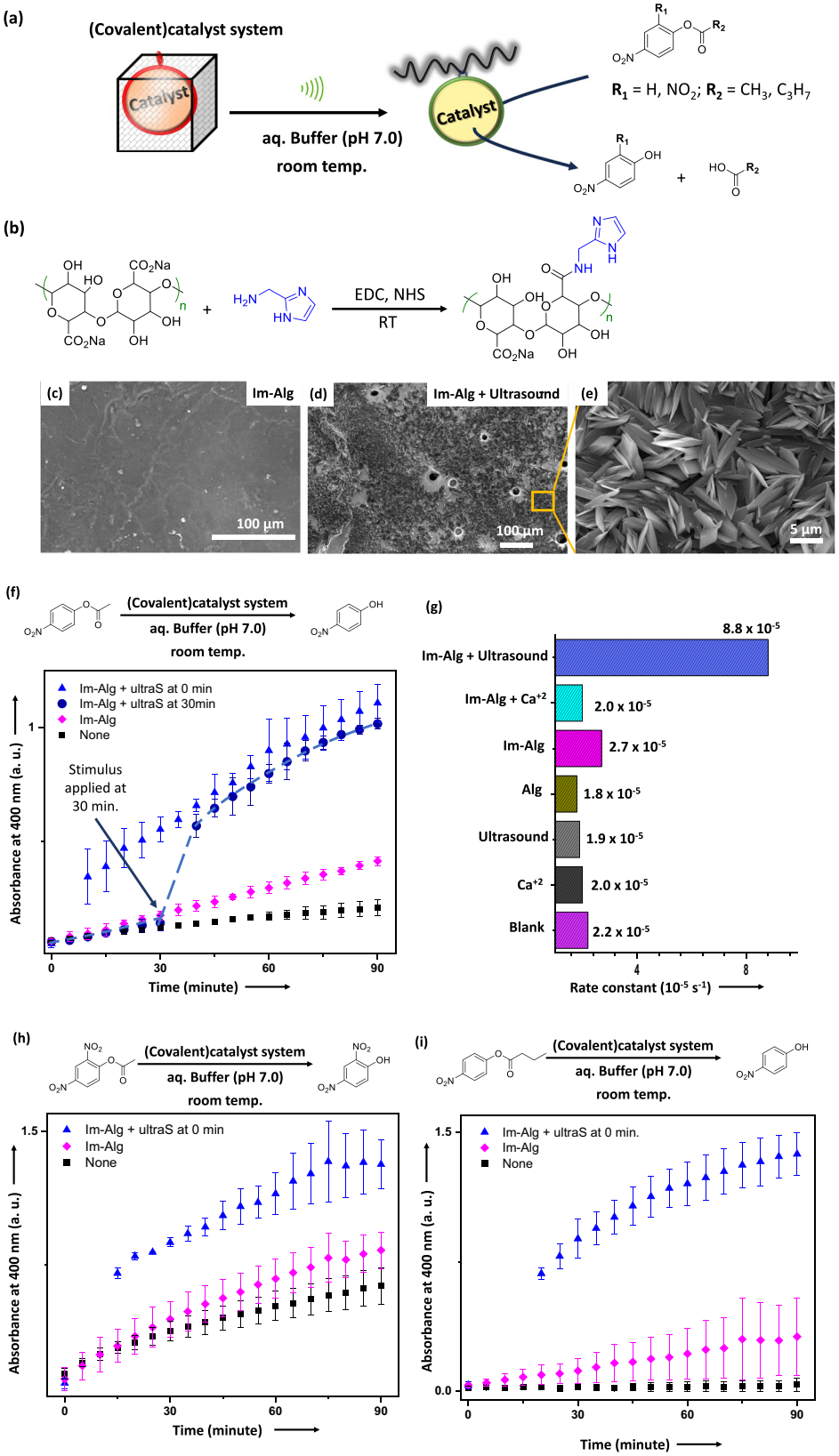

Fig. 3 | Ultrasound-controlled organocatalysis using (covalent)catalyst system in aqueous media. **a** A schematic of catalyst availability from the (covalent)catalyst system via the application of ultrasound stimulus for hydrolysis reaction of active esters in aqueous buffer at pH = 7.0, **b** Reaction scheme for imidazole-functionalized alginate (Im-Alg), (**c**–**e**) FESEM image of alginate material before (**c**) and after (**d**, **e**) the application of ultrasound stimulus. Scale bar is 100 µm (for **c**, **d**), and 5 µm (for **e**). **f**–**h** Controlled conversion for hydrolysis reaction in aqueous buffer (pH = 7.0). **f** Hydrolysis of pNPA in the presence of Im-Alg (magenta diamond), Im-Alg and ultrasound stimulus applied at the start of reaction (blue triangle), at 30 min (navy blue circle) and none (black square). The line is to guide the eyes. **g** Reaction rate constants for pNPA hydrolysis at different condition involving (covalent) catalyst system. **h** Hydrolysis of DNPA in the presence of Im-Alg (magenta diamond), Im-Alg and ultrasound stimulus applied at the start of reaction (blue triangle) and none (black square), **i** Hydrolysis of p-NPB in the presence of Im-Alg (magenta diamond), Im-Alg and ultrasound stimulus applied at the start of reaction (blue triangle) and none (black square). Markers indicates the experimental data. Error bars are based on standard errors in duplicate runs.

System design consideration

The degree of control over the aqueous organocatalysis is reduced due to the diffusional escape of the catalytic moiety from the hydrogel network. To this end, we envisioned that the diffusional escape could be restricted via the covalent attachment of the catalyst moiety to the alginate chain. The catalyst moiety would be only available via de-crosslinking of the alginate chains in the presence of ultrasound stimulus (covalent-catalyst system, Fig. 3a). For this, we have functionalized imidazole moiety covalently at the carboxyl group of alginate chains via carbodiimide activation (Fig. 3b). Addition of EDC (1-ethyl-3-(3-dimethylaminopropyl)carbodiimide),

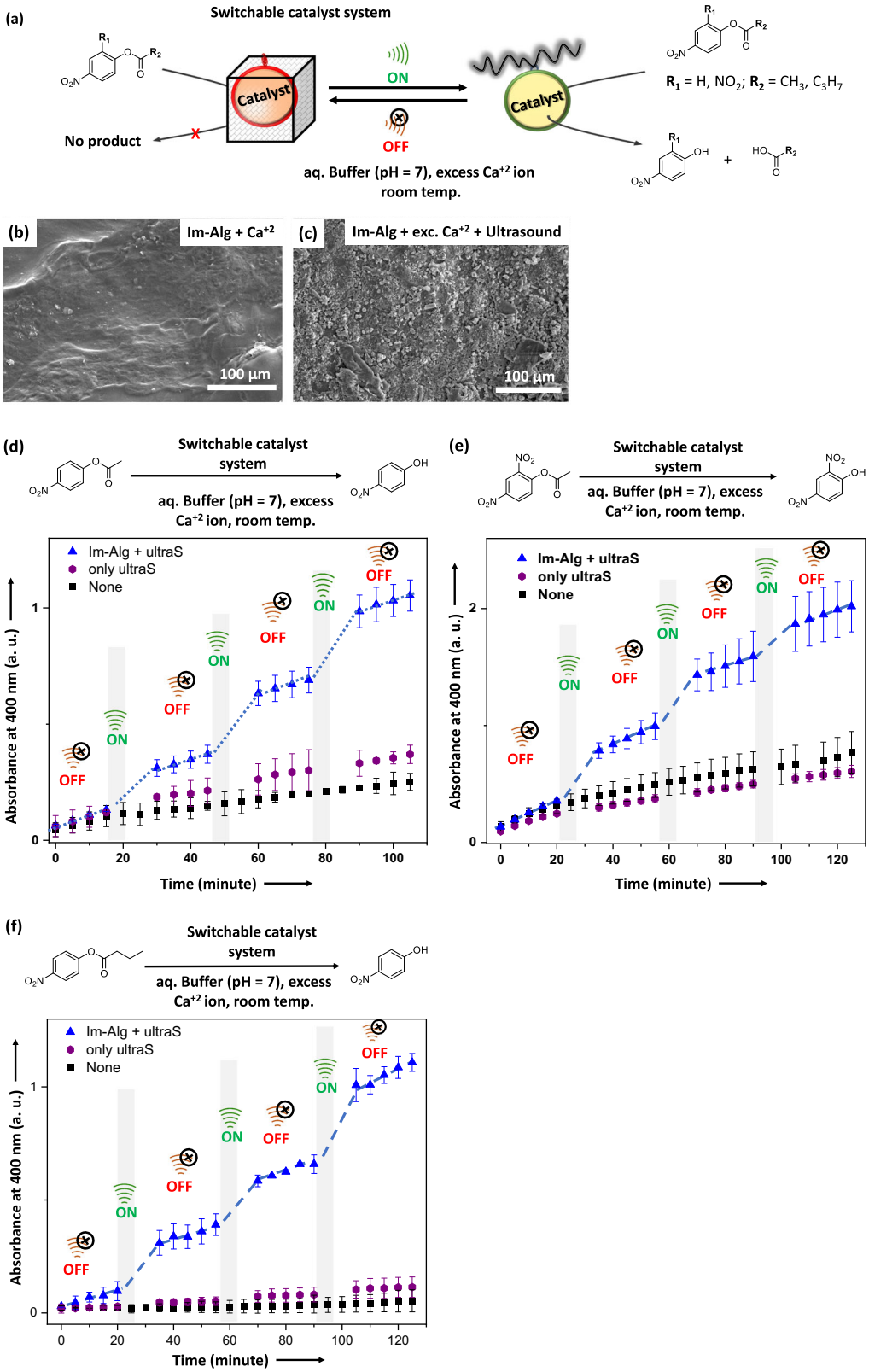

Fig. 4 | Ultrasound-induced reversible control over availability of organocatalyst for hydrolysis reaction in aqueous media. a A schematic of catalyst availability in the presence and absence of ultrasound stimulus in HEPES buffer containing Ca^{+2} ion, **b**, **c** FESEM micrograph of Im-Alg based material - before (**b**) and after (**c**) application of ultrasound in presence of Ca^{2+} ions, **d** conversion of pNPA in ambient conditions (blank, black square), in presence of ultrasound stimulus (purple hexagon), and in presence of Im-Alg and ultrasound stimulus (blue triangle), **e** conversion of DNPA in ambient conditions (blank, black square), in presence of ultrasound stimulus (purple hexagon), and in presence of Im-Alg and ultrasound stimulus (blue triangle), **f** conversion of pNPB in ambient conditions (blank, black square), in presence of ultrasound stimulus (purple hexagon), and in presence of Im-Alg and ultrasound stimulus (blue triangle). Ultrasound was employed during the course of the reaction at specific time for 5 min (ultrasound ON, shaded area) and ultrasound remain OFF for the remaining time. Markers indicates the experimental data. Error bars are based on standard errors in duplicate runs. The lines are to guide the eyes.

2-aminomethylimidazole, and NHS (N-hydroxysuccinimide) to the aqueous solution of sodium alginate resulted imidazole-functionalized alginate (Im-Alg, Supplementary Figs. S1–S3). Next, we prepared a stable opaque hydrogel material via dropwise addition of $CaCl_2$ to Im-Alg solution (3 wt%, similar concentration as previously employed). We obtained a uniform hydrogel material with Im-Alg using 50 mM $CaCl_2$ (no bead was obtained, and G'_{max} of the Im-Alg hydrogel material with 40 mM $CaCl_2$ was 7.0 kPa, Supplementary Fig. S4a, b). This is presumably due to modulation of the coordination sites in the alginate chains[37,48,49].

Next, we set out to examine the role of ultrasound on the Im-Alg-based hydrogel via FESEM study. Different micrographs were obtained before and after the application of ultrasound stimulus (Fig. 3c–e and Supplementary Fig. S3c–h). A homogeneous and smooth surface was observed for alginate material before ultrasound stimulus application (Fig. 3c), whereas a non-uniform surface having sharp-edged flake-like fragmentation, clusters and distinct hollow spheres were observed in FESEM image of alginate material after the application of ultrasound stimulus (Fig. 3d, e and Supplementary Fig. S3e, f). This confirmed the de-crosslinking of alginate chains in microscopic levels via ultrasound stimulus. Next, pNPA was added on top of the hydrogel material, and the progress of the reaction monitored via UV-Vis spectroscopy by taking aliquot at specific time interval (Fig. 3f). With Im-Alg and in the absence of ultrasound stimulus (magenta diamond, Fig. 3f), the hydrolysis reaction rate was $2.7 \times 10^{-5}\ s^{-1}$ (Fig. 3g), which was comparable with blank reaction (black square, Fig. 3f and rate = $2.2 \times 10^{-5}\ s^{-1}$, Fig. 3g). However, a 4-fold faster rate (Rate = $8.8 \times 10^{-5}\ s^{-1}$) was observed in presence of the ultrasound stimulus (blue triangle, Fig. 3f). This indicated ultrasound-induced availability of the catalyst moiety for the reaction. To rule out the contribution from other factors, we performed controlled experiments with pNPA in aqueous buffer solution (pH = 7.0). Experiments with only alginate (rate = $1.8 \times 10^{-5}\ s^{-1}$), the presence of excess Ca^{+2} ion (rate = $2.0 \times 10^{-5}\ s^{-1}$), or the presence of Im-Alg and Ca^{+2} ions (rate = $2.0 \times 10^{-5}\ s^{-1}$) (*vide infra*) provided similar rate constant as the blank reaction. Besides, the reaction rate (rate = $1.9 \times 10^{-5}\ s^{-1}$) did not improve via the application of ultrasound[50]. These results confirmed the role of ultrasound stimulus with the Im-Alg catalyst system for the availability of catalyst moiety. Next, we examined the change in reaction rate at any given time during the reaction via the addition of the ultrasound stimulus. We employed the ultrasound trigger after 30 min, showing an increase in reaction rate (navy blue circle, Fig. 3f). Besides, the reaction rate was similar as the background reaction during the initial 30 min. This result indicated the temporal response of the system to the stimulus from the environment. The availability of the imidazole catalyst to the pNPA substrate in the presence of ultrasound stimulus at any given time during the reaction, leading to a change in reaction rate at that particular moment. However, a slight increase in reaction rate (1.2-fold) in the absence of stimulus is presumably due to the diffusion of reactant molecules inside the alginate network. It is important to note that the reaction rate did not change after ceasing the ultrasound stimulus. Besides, no gel material was obtained, which was confirmed by vial inversion test. We measured the storage modulus of the viscous material (after the application of ultrasound stimulus), and a G'_{max} was obtained as 1.8 kPa (Supplementary Fig. S4a, b). This indicated the loss of Ca^{+2} ion in the reaction medium due to the application of ultrasound, resulting inefficient re-crosslinking of the alginate chains.

The versatility of the Im-Alg material as an ultrasound-responsive catalyst system become more apparent as we additionally examined the hydrolysis of other activated ester derivatives (2,4-dinitrophenyl acetate, DNPA[51] and *para*-nitrophenyl butyrate, pNPB). Following the UV-vis absorption study at 400 nm, we observed a pseudo-first-order reaction (rate constant = $31.9 \times 10^{-5}\ s^{-1}$) for the formation of dinitrophenol from DNPA (Fig. 3h) employing the stimulus (ultrasound at the beginning, blue triangle). In the absence of stimulus, the rate constant was $18.1 \times 10^{-5}\ s^{-1}$ (magenta diamond), which was 2.8-fold higher than the blank reaction (rate = $6.5 \times 10^{-5}\ s^{-1}$, black square). This is due to the higher activity of DNPA in aqueous medium[52], and diffusion of the substrate in the alginate network, facilitating its hydrolysis. In comparison, we examined the hydrolysis rate of pNPB in similar conditions (Fig. 3i). The hydrolysis of pNPB displayed a lower hydrolysis rate in blank condition (rate = $0.8 \times 10^{-5}\ s^{-1}$, black square). This is presumably due to the formation of micellar structure in aqueous media by the hydrophobic pNPB substrate, resulting inhibition of the ester hydrolysis. However, a 6.1-fold higher reaction was observed in the presence of Im-Alg material (rate = $4.9 \times 10^{-5}\ s^{-1}$, magenta diamond), indicating the diffusion of the pNPB inside the alginate network. Interestingly, the system displayed a remarkable 51.1 times higher rate ($40.9 \times 10^{-5}\ s^{-1}$, blue triangle) in the presence of ultrasound stimulus, implying the effectiveness of ultrasound-induced catalyst availability via de-crosslinking the alginate chains. Altogether, we shown that control over the reaction rate of ester hydrolysis is feasible via using Im-Alg-based covalent-catalytic system and the application of ultrasound stimulus in aqueous media. Additionally, the application of ultrasound at any given time during the reaction led changing the reaction rate at that particular moment.

Reversible control over aqueous organocatalysis

Reversible control over organocatalysis using ultrasound-induced de-crosslinking of Im-Alg and re-crosslinking in absence of the trigger was investigated next. We used excess Ca^{+2} ions in the reaction medium by incorporating $CaCl_2$ (50 mM) in HEPES buffer (pH = 7) (similar concentration of Ca^{+2} ions used for Im-Alg material preparation, see Supplementary Table S3). This would allow the availability of imidazole only after de-crosslinking of the alginate network via the application of ultrasound stimulus, whereas excess amount of Ca^{+2} ions in the reaction medium would allow re-crosslinking of the alginate in the absence of ultrasound stimulus (Fig. 4a). Indeed, in presence of excess Ca^{+2} ions in the medium, we obtained hydrogel material after switching OFF the ultrasound stimulus. We measured the storage modulus of the obtained gel material, which showed similar rheology behaviour as the parent Im-Alg hydrogel material (Supplementary Fig. S4a). A G'_{max} of 7.7 kPa was obtained for the re-formed gel in comparison to the G'_{max} (7.0 kPa) of the parent Im-Alg material (Supplementary Fig. S4b). This indicated re-crosslinking of the alginate chains after ceasing the ultrasound stimulus. Next, we recorded the FESEM of Im-Alg materials obtained from a solution having Im-Alg hydrogel material in HEPES buffer containing excess Ca^{+2} ions (50 mM). A homogeneous surface with uniform morphology was observed for the Im-Alg material where no ultrasound stimulus was applied (Fig. 4b), whereas a non-smooth surface was observed for the Im-Alg material, where ultrasound stimulus was applied in the mixture having excess of Ca^{+2} ions in buffer solution (Fig. 4c). Absence of any sharp-edged particles or hollow objects implies re-crosslinking of alginate chains in presence of excess Ca^{+2} ions when the ultrasound was ceased. This indicates that de-crosslinking and re-crosslinking of the alginate chains are feasible by applying and ceasing ultrasound stimulus in the solution having excess crosslinking (Ca^{+2}) ions.

Next, we performed hydrolysis with Im-Alg material in HEPES buffer having an excess of Ca^{+2} ions (pH = 7.0). We first examined the reversible control over the pNPA hydrolysis (Fig. 4d). We observed Ca^{+2}-crosslinked alginate network in the absence of an ultrasound trigger, resulting 'OFF' state of the catalytic reaction for the first 15 min (Fig. 4d, blue triangle), which is comparable to background reaction (black square, Fig. 4d). An increase in reaction rate was observed after application of ultrasound trigger for 5 min (shaded region, Fig. 4d), whereas the reaction rate become similar as blank reaction in absence of the stimulus. This indicates that the catalysis is 'ON' in the presence of an ultrasound trigger due to the de-crosslinking of alginate chains, whereas the re-crosslinking in the presence of Ca^{+2} ions lead to catalysis 'OFF'. Interestingly, conversion of the reaction only in the presence of an ultrasound trigger did not increase the reaction rate (purple hexagon, Fig. 4d), indicating negligible contribution of ultrasound for the hydrolysis reaction. It is worth noting that absorbance measurement was done after 10 min of the application of ultrasound due to technical issue. In consecutive cycles, the application of stimulus for 5 min resulted an increase

in reaction rate, whereas, indifferent reaction rate was observed in the absence of stimulus. This result indicated that control over aqueous catalysis between 'ON' and 'OFF' state is feasible employing ultrasound as stimulus. We also examined the reversible control over the hydrolysis reaction of DNPA and pNPB. We observed similar behaviour in reaction rates for the hydrolysis of DNPA (Fig. 4e, blue triangle), and pNPB (Fig. 4f, blue triangle) on exposure to fixed durations of repeated ultrasound stimulus. In the absence of the stimulus, the reaction rate was similar as the background reaction (black rectangle, Fig. 4e for DNPA and Fig. 4f for pNPB). In addition, the effect of ultrasound was examined without the catalyst system. We did not observe any significant increase in the reaction rate (purple hexagon, Fig. 4e for DNPA and Fig. 4f for pNPB), demonstrating the reaction is specific for the catalytic action. However, we observed a lower reaction rate of DNPA in the presence of excess Ca^{+2} ion and ultrasound stimulus, compared to the blank reaction (Fig. 4e). This is presumably due to shielding the ultrasound energy by an ionic interaction between Ca^{+2} ion and DNPA. It is worth mentioning that the presence of excess Ca^{+2} ions in HEPES buffer did not influence the hydrolysis reaction for all three ester substrates (Fig. 3g, Entry 4 in Supplementary Table S6, and Entry 4 in Supplementary Table S7). Altogether, Im-Alg-based catalyst system would allow 'ON/OFF' control over the catalysis in aqueous media via the presence or absence of the ultrasound stimulus.

Discussion

In conclusion, we have successfully demonstrated control over aqueous organocatalysis via the application of ultrasound stimulus. Alginate biopolymer that is capable of forming hydrogels can encapsulate imidazole as an organocatalytic moiety non-covalently within its network (non-covalent-catalyst system). The organocatalysis would be 'OFF' due to the inaccessibility of the catalytic site to the substrates. Application of ultrasound stimulus would allow 'ON' state of the catalytic system, enabling the access of the ester substrates to imidazole for hydrolysis reaction. The system shows the temporal accessibility of entrapped catalytic species via application of the ultrasound stimulus at any time during the reaction. However, the diffusional escape of catalytic moiety from the hydrogel network reduces the degree of control over the aqueous organocatalysis. The issue is addressed by attaching the catalytic moiety with the alginate chain (covalent-catalyst system). Incorporation of imidazole moiety with the alginate network minimized the diffusional escape of the catalytic moiety and thereby provides better control over the system. The catalyst centre could be accessible at any moment during the reaction, allowing temporal control over the reaction via the presence of ultrasound stimulus. The versatility of the catalyst system was demonstrated by using several activated esters as substrates. Besides, we have shown the reversible control over aqueous organocatalysis by applying ultrasound stimulus or by ceasing it. We use excess Ca^{+2} ions in the reaction media, allowing efficient re-crosslinking of the alginate chains after ceasing the ultrasound stimulus. We also demonstrate the switching 'ON' and 'OFF' the organocatalysis in the aqueous media. Application of ultrasound stimulus de-crosslinks the alginate network, enabling organocatalysis 'ON', whereas ceasing the ultrasound re-crosslinks the alginate network in the presence of excess Ca^{+2} ion present in the media, results organocatalysis 'OFF'.

The developed approach of ultrasound-triggered organocatalysis can be used for controlled and 'on-demand' formation of organic compounds in aqueous media. The system would further be employed for any reaction in aqueous media using the desired catalytic moiety. In addition, the system could be coupled with supramolecular self-assembly to obtain 'on-demand' material with spatiotemporal control. Upgradation of the system could allow reversibly control over certain functionality just by switching 'ON' and 'OFF' the ultrasound stimulus.

Methods

Preparation of alginate material

For determining the amount of Ca^{+2} ions required for alginate gel material, a solution of $CaCl_2$ was added dropwise to an alginate solution unless a colourless gel is observed. Gelation is confirmed by inversion vial test. Alginate biopolymer or organocatalyst functionalized alginate materials were prepared by dropwise adding $CaCl_2$ solution to the corresponding alginate solution (3 wt%, at a concentration above the determined minimum crosslinking ion concentration). For non-covalent entrapment of organocatalysts, imidazole (0.25 mM) was mixed with alginate solution, followed by the preparation of a homogeneous solution and the addition of Ca^{+2} ions for crosslinking.

Application of ultrasound stimulus

Ultrasound-induced reaction was performed via providing sonication signal to the reactant solution in the presence of alginate material having organocatalytic moiety with probe sonicator having frequency range of 20–25 kHz (auto-tracking, 650 W, 220 V/50 Hz, Model No. PRO-650, serial no. L35435, LABMAN) for a period of 5 min. The temperature was maintained constant at ambient condition (25–30 °C) before, during and after the sonication cycles (water bath was used to maintain temperature and replaced after regular intervals to drain out the heat released). For control over catalytic action, the reaction mixture was allowed to react at ambient condition (uncatalyzed version). After the desired time, ultrasound energy was provided, followed by recording UV-Vis spectral data. We also recorded the reaction progress in the presence of all associated components and variables without the ultrasound stimulus.

Rheological measurements

All hydrogels were prepared using sodium alginate (3 wt%) with optimized CaCl2 concentration (40 mM) in suitable vials and once definite stability is reached, it is transferred to the lower plate of the geometry (parallel plate, 25 mm diameter). Thereafter, the upper plate is lowered maintaining a gap height of 0.5 mm and the excess of the gel material is cut off with a knife or spatula. The storage modulus (G′) and loss modulus (G″) of the hydrogels under test were then obtained under strain-controlled conditions (fixed at 1% strain) in oscillating frequency range of 0.1–100.0 rad/s. For analysing systems with entrapped catalysts, similar imidazole concentrations were used as previous experiments.

Measurement of catalytic activity

Hydrolysis of the activated esters (pNPA, p-NPB, and DNPA) was carried out as bond breaking reaction in aqueous media. As control experiment, the reaction was followed via UV-visible absorption spectrometer in the presence of imidazole or Im-Alg (organocatalyzed reaction) and the absence of imidazole (control uncatalyzed reaction). For all ester reaction cycles, a solution of the substrate (pNPA/pNPB/DNPA, 0.5 mM, 1eq) in DMF was dispersed in HEPES buffer (pH 7.0, 1:9 ratio) (DMF/HEPES buffer), at ambient conditions. The hydrolysis reaction was monitored via UV-Vis spectroscopy. For determining the rate constants, the product formation (p-nitrophenol or dinitrophenol) was followed by recording the absorbance at 400 nm at regular intervals. The pseudo-first-order rate constant (**k**) has obtained by plotting $\mathbf{A_t}$ (absorbance at 400 nm at time '**t**') as the dependent variable and time (**t**) as independent variable, followed by best fit curve in Origin 2022 (Box Lucas fit).

Data availability

The datasets generated during the current study are available from the corresponding author on reasonable request.

Received: 27 March 2024; Accepted: 13 September 2024;
Published online: 30 September 2024

References

1. Hafen, E. Kinases and phosphatases – a marriage is consummated. *Science* **280**, 1212 (1998).
2. Kovbasyuk, L. & Krämer, R. Allosteric supramolecular receptors and catalysts. *Chem. Rev.* **104**, 3161 (2004).

3. Eelkema, R. & van Esch, J. H. Catalytic control over the formation of supramolecular materials. *Org. Biomol. Chem.* **12**, 6292–6296 (2014).
4. Blanco, V., Leigh, D. A. & Marcos, V. Artificial switchable catalysts. *Chem. Soc. Rev.* **44**, 5341 (2015).
5. Wei, W., Zhu, M., Wu, S., Shen, X. & Li, S. Stimuli-responsive biopolymers: an inspiration for synthetic smart materials and their applications in self-controlled catalysis. *J. Inorg. Organomet. Polym.* **30**, 69–87 (2020).
6. Cortes-Clerget, M. et al. Water as the reaction medium in organic chemistry: from our worst enemy to our best friend. *Chem. Sci.* **12**, 4237–4266 (2021).
7. Kitanosono, T., Masuda, K., Xu, P. & Kobayashi, S. Catalytic organic reactions in water toward sustainable society. *Chem. Rev.* **118**, 679–746 (2018).
8. van der Helm, M. P., Klemm, B. & Eelkema, R. Organocatalysis in aqueous media. *Nat. Rev. Chem.* **3**, 491–508 (2019).
9. Das, N. & Maity, C. Chemical transformations in supramolecular hydrogels. *ACS Catal.* **13**, 5544–5570 (2023).
10. Das, N. & Maity, C. Switchable aqueous catalytic systems for organic transformations. *Commun. Chem.* **5**, 115 (2022).
11. He, X. et al. Synthetic homeostatic materials with chemo-mechano-chemical self-regulation. *Nature* **487**, 214–218 (2012).
12. Zayas, H. A. et al. Thermoresponsive polymer-supported L-proline micelle catalysts for the direct asymmetric aldol reaction in water. *ACS Macro Lett.* **2**, 327–331 (2013).
13. Kuepfert, M., Ahmed, E. & Weck, M. Self-assembled thermoresponsive molecular brushes as nanoreactors for asymmetric aldol addition in water. *Macromolecules* **54**, 3845–3853 (2021).
14. Zhang, C. et al. Switchable hydrolase based on reversible formation of supramolecular catalytic site using a self-assembling peptide. *Angew. Chem. Int. Ed.* **56**, 14511–14515 (2017).
15. Arlegui, A., Torres, P., Cuesta, V., Crusats, J. & Moyano, A. A pH-switchable aqueous organocatalysis with amphiphilic secondary amine–porphyrin hybrids. *Eur. J. Org. Chem.* **2020**, 4399–4407 (2020).
16. Yang, H., Zhou, T. & Zhang, W. A strategy for separating and recycling solid catalysts based on the pH-triggered pickering-emulsion inversion. *Angew. Chem. Int. Ed.* **52**, 7455–7459 (2013).
17. Wilson, D. & Branda, N. R. Turning "On" and "Off" a pyridoxal 5'-phosphate mimic using light. *Angew. Chem. Int. Ed.* **51**, 5431–5434 (2012).
18. Lee, W.-S. & Ueno, A. Photocontrol of the catalytic activity of a β-cyclodextrin bearing azobenzene and histidine moieties as a pendant group. *Macromol. Rapid Commun.* **22**, 448–450 (2001).
19. Zhao, Y. et al. A supramolecular approach to construct a hydrolase mimic with photo-switchable catalytic activity. *J. Mater. Chem. B* **6**, 2444–2449 (2018).
20. Saha, M. & Bandyopadhyay, S. A reversible photoresponsive activity of a carbonic anhydrase mimic. *Chem. Commun.* **55**, 3294–3297 (2019).
21. Ren, C. Z.-J., Muñana, P. S., Dupont, J., Zhou, S. S. & Chen, J. L.-Y. Reversible formation of a light-responsive catalyst by utilizing intermolecular cooperative effects. *Angew. Chem. Int. Ed.* **58**, 15254 (2019).
22. Zhao, H. et al. Reversible trapping and reaction acceleration within dynamically self-assembling nanoflasks. *Nat. Nanotech.* **11**, 82–88 (2016).
23. Li, Z. et al. Light-switched reversible emulsification and demulsification of oil-in-water Pickering emulsions. *Angew. Chem. Int. Ed.* **60**, 3928–3933 (2021).
24. Groote, R., Jakobs, R. T. M. & Sijbesma, R. P. Mechanocatalysis: forcing latent catalysts into action. *Polym. Chem.* **4**, 4846 (2013).
25. Li, J., Nagamani, C. & Moore, J. S. Polymer mechanochemistry: from destructive to productive. *Acc. Chem. Res.* **48**, 2181–2190 (2015).
26. Piermattei, A., Karthikeyan, S. & Sijbesma, R. P. Activating catalysts with mechanical force. *Nat. Chem.* **1**, 133–137 (2009).
27. Karthikeyan, S., Potisek, S. L., Piermattei, A. & Sijbesma, R. P. Highly efficient mechanochemical scission of silver-carbene coordination polymers. *J. Am. Chem. Soc.* **130**, 14968–14969 (2008).
28. Moyano, A. & Crusats, J. Multi-length scale communication effects in catalysis: thinking big and acting small. *Adv. Synth. Catal.* **366**, 617–634 (2024).
29. O'Neill, R. T. & Boulatov, R. The many flavours of mechanochemistry and its plausible conceptual underpinnings. *Nat. Rev. Chem.* **5**, 148–167 (2021).
30. Huo, S. et al. Mechanochemical bond scission for the activation of drugs. *Nat. Chem.* **13**, 131–139 (2021).
31. Versaw, B. A., Zeng, T., Hu, X. & Robb, M. J. Harnessing the power of force: development of mechanophores for molecular release. *J. Am. Chem. Soc.* **143**, 21461–21473 (2021).
32. Klok, H.-A., Herrmann, A. & Göstl, R. Force ahead: emerging applications and opportunities of polymer mechanochemistry. *ACS Polym. Au* **2**, 208–212 (2022).
33. Das, A. & Datta, A. Designing site specificity in the mechanochemical cargo release of small molecules. *J. Am. Chem. Soc.* **145**, 13484–13490 (2023).
34. Sun, Y. et al. Mechanically triggered carbon monoxide release with turn-on aggregation-induced emission. *J. Am. Chem. Soc.* **144**, 1125–1129 (2022).
35. Meissner, S. et al. Investigating the influence of ultrasound parameters on ibuprofen drug release from hydrogels. *Drug Deliv. Transl. Res.* **13**, 1390–1404 (2023).
36. Emi, T. et al. Ultrasonic generation of pulsatile and sequential therapeutic delivery profiles from calcium-crosslinked alginate hydrogels. *Molecules* **24**, 1048 (2019).
37. Maity, C. & Das, N. Alginate-based smart materials and their application: recent advances and perspectives. *Top. Curr. Chem.* **380**, 3 (2022).
38. Huebsch, N. et al. Ultrasound-triggered disruption and self-healing of reversibly cross-linked hydrogels for drug delivery and enhanced chemotherapy. *Proc. Natl Acad. Sci. USA* **111**, 9762–9767 (2014).
39. Cao, L., Lu, W., Mata, A., Nishinari, K. & Fang, Y. Egg-box model-based gelation of alginate and pectin: a review. *Carbohydr. Polym.* **242**, 116389 (2020).
40. Ramdhan, T., Ching, S. H., Prakash, S. & Bhandari, B. Time dependent gelling properties of cuboid alginate gels made by external gelation method: effects of alginate-$CaCl_2$ solution ratios and pH. *Food Hydrocoll.* **90**, 232–240 (2019).
41. Pérez-Madrigal, M. M. et al. A paradigm shift for preparing versatile M^{2+}-free gels from unmodified sodium alginate. *Biomacromolecules* **18**, 2967–2979 (2017).
42. Wang, M., Zhang, Z. & Zhang, W. Design, synthesis, and application of chiral bicyclic imidazole catalysts. *Acc. Chem. Res.* **55**, 2708–2727 (2022).
43. Tilly, D. P., Heeb, J.-P., Webb, S. J. & Clayden, J. Switching imidazole reactivity by dynamic control of tautomer state in an allosteric foldamer. *Nat. Commun.* **14**, 2647 (2023).
44. Soreq, H. & Seidman, S. Acetylcholinesterase—new roles for an old actor. *Nat. Rev. Neurosci.* **2**, 294–302 (2001).
45. Nieri, P. et al. Cholinesterase-like organocatalysis by imidazole and imidazole-bearing molecules. *Sci. Rep.* **8**, 45760 (2017).
46. Bruice, T. C. & Schmir, G. L. Imidazole catalysis. II. The reaction of substituted imidazoles with phenyl acetates in aqueous Solution. *J. Am. Chem. Soc.* **80**, 148–156 (1958).
47. Bender, M. L. & Turnquest, B. W. The imidazole-catalyzed hydrolysis of p-nitrophenyl acetate. *J. Am. Chem. Soc.* **79**, 1652–1655 (1957).
48. Roquero, D. M., Othman, A., Melman, A. & Katz, E. Iron(iii)-cross-linked alginate hydrogels: a critical review. *Mater. Adv.* **3**, 1849–1873 (2022).
49. Shen, K.-H., Yeh, Y.-Y., Chiu, T.-H., Wang, R. & Yeh, Y.-C. Dual dynamic covalently crosslinked alginate hydrogels with tunable

properties and multiple stimuli-responsiveness. *ACS Biomater. Sci. Eng.* **8**, 4249–4261 (2022).
50. Martínez, R. F., Cravotto, G. & Cintas, P. Organic sonochemistry: a chemist's timely perspective on mechanisms and reactivity. *J. Org. Chem.* **86**, 13833–13856 (2021).
51. Guler, M. O. & Stupp, S. I. A self-assembled nanofiber catalyst for ester hydrolysis. *J. Am. Chem. Soc.* **129**, 12082–12083 (2007).
52. Castro, E. A. & Ureta, C. Kinetics and mechanism of the reactions of 2,4-dinitrophenyl acetate with secondary alicyclic amines. Different nucleofugalities of alicyclic amines and pyridines from a tetrahedral intermediate. *J. Org. Chem.* **55**, 1676–1679 (1990).

Acknowledgements

C.M. acknowledges the financial support from the Science and Engineering Research Board (SERB) as Start-up research grant (No. – SRG/2020/000571). N.D. thanks DST for INSPIRE fellowship (No. – DST/INSPIRE/03/2022/000179). Authors acknowledge the instrumentation facility at VIT Vellore to carry out this research work. We thank Prof. Suryasarathi Bose and Mr. Samir Mandal (IISC, Bangalore) for allowing to carry out rheology measurements of the materials.

Author contributions

C.M. conceived the research idea. N.D. and C.M. designed the research, and N.D. carried out the experiments. C.M. directed the research. C.M. and N.D. wrote the manuscript. All authors commented on the work and the manuscript.

Funding

Open access funding provided by Vellore Institute of Technology.

Competing interests

The authors declare no competing interests.

Additional information

Supplementary information The online version contains supplementary material available at https://doi.org/10.1038/s43246-024-00640-y.

Correspondence and requests for materials should be addressed to Chandan Maity.

Peer review information *Communications materials* thanks Zhanhua Wang and the other, anonymous, reviewer(s) for their contribution to the peer review of this work. Primary Handling Editors: Jet-Sing Lee. A peer review file is available.